Keto-enol Tautomers of Mixed-Ligand Ruthenium(II) Complexes Containing α-Diamine and Azoimine Bearing Alkyne Group Ligands

Mousa Al-Noaimi, Ayman Hammoudeh, Mohammad El-khateeb, Firas F. Awwadi, Deeb Taher, Ahmad Mansi, Obadah S. Abdel-Rahman

PII: S0020-1693(16)30195-5
DOI: http://dx.doi.org/10.1016/j.ica.2016.04.029
Reference: ICA 17013

To appear in: *Inorganica Chimica Acta*

Received Date: 16 February 2016
Revised Date: 12 April 2016
Accepted Date: 15 April 2016

Please cite this article as: M. Al-Noaimi, A. Hammoudeh, M. El-khateeb, F.F. Awwadi, D. Taher, A. Mansi, O.S. Abdel-Rahman, Keto-enol Tautomers of Mixed-Ligand Ruthenium(II) Complexes Containing α-Diamine and Azoimine Bearing Alkyne Group Ligands, *Inorganica Chimica Acta* (2016), doi: http://dx.doi.org/10.1016/j.ica.2016.04.029

Keto-enol Tautomers of Mixed-Ligand Ruthenium(II) Complexes Containing α-Diamine and Azoimine Bearing Alkyne Group Ligands

Mousa Al-Noaimi[a]*, Ayman Hammoudeh[b], Mohammad El-khateeb[c], Firas F. Awwadi[d], Deeb Taher[d], Ahmad Mansi[a], Obadah S. Abdel-Rahman[e]

[a]Department of Chemistry, Hashemite University, P.O. Box 150459, Zarqa-13115-Jordan

[b]Department of Chemistry, Yarmouk University, P.O. Box 566, Irbid, Jordan

[c]Department of Chemistry, Jordan University of Science and Technology, Irbid 22110, Jordan

[d]Department of Chemistry, The University of Jordan, Amman 11942, Jordan

[e]Fachbereich Chemie der Universität Konstanz, Universitätstraße 10, D-78457 Konstanz, Germany

Abstract

Refluxing azoimine ligand containing terminal acetylene group (L= $C_6H_5N=NC(COCH_3)=NC_6H_4C\equiv CH$) with $RuCl_3.3H_2O$ in ethanol resulted hydrating the terminal acetylene group to the corresponding enol form $C_6H_5N=N-C(COCH_3)=NC_6H_4C(OH)=CH_2$ (L1), ketone form $C_6H_5N=NC(COCH_3)=NC_6H_4COCH_3$ (L2) and vinyl chloride: $C_6H_5N=N=C(COCH_3)=N–C_6H_4C(Cl)=CH_2$ (L3) *via* Markovnikov selectivity. Ruthenium complexes of the later ligands and α-diamines of the formula *trans*-[Ru(N-N)(Y)Cl_2] (Y = L1, N-N = 4,4'-dimethoxy-2,2'-bipyridine; dmeb (**1**), 1,10-phenanthroline; phen (**2**), 3,4,7,8-tetramethyl-1,10-phenanthroline; tmphen (**3**), Y = L2, N-N = dmeb (**4**), phen (**5**), tmphen (**6**)) were synthesized from L, N-N ligands and $RuCl_3.3H_2O$. Complexes **1-6** were characterized by spectroscopic (IR, UV–Vis, ^{1}H-, ^{13}C-NMR, DEPT-135) and electrochemistry techniques. The crystal structures of *trans*-[Ru(tmphen)(L1)Cl_2] (**3**) and *trans*-[Ru(bpy)(L3)Cl_2] (**7**) were determined and found to have distorted octahedral geometry. The catalytic activity of **3** towards the hydration of cinnamaldehyde is reported.

Key words: Ruthenium, Catalytic Hydration, Keto-enol tautomers, Spectroelectrochemistry, Electrochemistry.

---

*Corresponding authors. Fax: +962 (5) 3826613.

E–mail address: manoaimi@hu.edu.jo (M. Al-Noaimi)

1. Introduction

The addition of water to the triple bond of non-activated alkynes, in presence of electrophilic catalysts, results in the formation of carbonyl derivatives [1-3]. Historically, mercuric ions in dilute acidic conditions were used as catalysts for the synthesis of ketones from terminal and internal alkynes [3]. Due to the environmental concerns of mercury, other transition-metal-complexes such as Au(I) [1,2], Ru(III) [4], Rh(II) [5], Pd(II) [6], Os(II) [7] and other metals [8, 9] have been used. For instance, when phenylacetylene and *p*-toluene sulfonic acid were reacted, in dichloromethane in the presence of catalytic amount of $FeCl_3$, acetophenone was selectively obtained in a good yield in addition to 2-vinyl chlride as a by-product [9]. Ru(II) complexes, in the presence of appropriate auxiliary phosphine ligands, have efficiently catalyzed the anti-Markovnikov addition of oxygen to terminal alkynes, yielding mainly aldehydes [10].

As part of our continuing interest in the ruthenium azoimine chemistry [11-15], we synthesized the terminal acetylene azoimine ligand $C_6H_5NH\text{-}N{=}C(COCH_3)NHC_6H_4C{\equiv}CH$ (L) [15]. When L reacted with $RuCl_3.3H_2O$, the terminal acetylene group of the ligand (L) was catalytically hydrated *via* Markovnikov addition to the corresponding enol (L1) and keto (L2) forms. Two mixed-ligand complexes, *trans*-$[Ru(bpy)(L1)Cl_2]$ and $[Ru(bpy)(L2)Cl_2]$, were prepared and characterized [18]. In this work, mixed-ligand ruthenium complexes with α-diamines (N-N = 1,10-phenanthroline (phen), 4,4'-dimethoxy-2,2'-bipyridine (dmeb), 3,4,7,8-tetramethyl-1,10-phenanthroline (tmphen)) having the general formula *trans*-$[Ru(N\text{-}N)(Y)Cl_2]$ (**1-6**) (Y =L1, L2) were prepared to study the effect of the N-N ligands on the electronic properties of the ruthenium center. The effect of the substituents on the N-N ligands will be monitored by the shift of the Ru(III/II) couple and the low energy metal-ligand charge transfer for these complexes. Complex **3** will be investigated as a catalyst in the hydrogenation of cinnamaldehyde.

2. Experimental

2.1. Materials

Ruthenium trichloride trihydrate ($RuCl_3.3H_2O$), 1,10-phenanthroline (phen), 4,4'-dimethoxy-2,2'-bipyridine (dmeb), 3,4,7,8-tetramethyl-1,10-phenanthroline (tmphen), tetrabutylammonium hexafluorophosphate ($TBAPF_6$) were purchased from Aldrich. C_6H_5–NHN=C($COCH_3$)$NHC_6H_4C{\equiv}CH$ (L) was prepared following the reported procedure [15].

2.2. General Procedure for the Preparation of trans-[Ru(N-N)(L)(Cl_2)](**1-6**);

$RuCl_3.3H_2O$ (0.27 g, 1.0 mmol) and the ligand L (0.25 g, 1.0 mmol) were dissolved in 100 mL of absolute ethanol. The mixture was refluxed for 1 h after which 1.0 mmol of (N-N) ligand was added to the solution. The reaction mixture was refluxed for additional 2 h then the solvent was removed under reduced pressure. The volume of the reaction mixture was reduced to *ca*. 20 mL and then diethyl ether was added to precipitate the product. The product was dissolved in a minimum volume of CH_2Cl_2 and subjected to chromatographic separation on a silica gel column (60–120 mesh). Red bands of the [Ru(bpy)(L3)Cl_2] (**7**), *trans*-[Ru(N-N)(L1)Cl_2] (**1-3**) and *trans*-[Ru(N-N)(L2)Cl_2] (**4-6**) were obtained by gradually increase the amount of acetone as mobile phase from the mixture of 3:1 (V:V) of acetone/hexane to pure acetone. Upon slow evaporation of the solvent a few red crystals of complexes **3** and **7** were found. Complex 7 was obtained only in a trace amount and characterized only by x-ray structure determination.

2.2.1.trans-[Ru(dmeb)(L1)Cl_2] (**1**): Yield: 0.17 g (25%). Anal. Calcd. for $C_{29}H_{27}Cl_2N_5O_4Ru$: C, 51.11; H, 3.99; N, 10.28. Found: C, 51.16; H, 4.05; N, 10.34. UV-Vis in CH_2Cl_2 [λ_{max}/nm (ε_{max}/ $M^{-1}cm^{-1}$)]: 256 (26.13×10^3), 313 (16.18×10^3), 389 (6.53×10^3), 505 (4.70×10^3). IR (KBr, cm^{-1}): 1449 (*v* N=N), 1590 (*v* C=N), 1691(*v* C=O). ^{1}H-NMR (300

MHz, $CDCl_3$): 8.08 (2H, d, H3), 7.73 (3H, m, H4, H5), 7.58 (3H, m, dmeb), 7.54 (1H, d, H1), 7.40 (2H, d, H2), 6.93 (1H, d, dmeb), 6.5 (2H, m, dmeb), 5.93 (1H, s, $=CH_a$), 5.67 (1H, s, $=CH_b$), 4.70 (1H, s, C(O<u>H</u>)=C), 3.93 (3H, s, OCH_3), 3.92 (3H, s, OCH_3), 2.84 (3H, s, $COCH_3$). ^{13}C-NMR (300 MHz, $CDCl_3$): 189.1(C=O), 135.3 (<u>C</u>(OH)=C), 113.0 ($=\underline{C}H_2$), 56.17 (OCH_3), 56.14 (OCH_3) , 30.2, ($COCH_3$).

2.2.2. trans-[Ru(phen)(L1)Cl$_2$] (**2**)*:* Yield: 0.141 g (22%). Anal. Calcd. for $C_{29}H_{23}Cl_2N_5O_2Ru$: C, 53.96; H, 3.59; N, 10.85. Found: C, 53.85; H, 3.62; N, 10.90. UV-Vis in CH_2Cl_2 [λ_{max}/nm (ε_{max}/ $M^{-1}cm^{-1}$)]: 316 (26.65×10^3), 379 (15.72×10^3), 510 (12.09×10^3). IR (KBr, cm^{-1}): 1448 (*v* N=N), 1591 (*v* C=N), 1701 (*v* C=O). ^{1}H-NMR (300 MHz, $CDCl_3$): 8.34 (1H, d, phen), 8.32 (1H, d, phen), 8.18 (3H, m, H3, phen), 7.97 (1H, d, phen), 7.87 (2H, d, H1), 7.79 (1H, t, H5), 7.71 (2H, d, H2), 7.61 (2H, t, H4), 7.58 (4H, m, phen), 5.94 (1H, s, $=CH_a$), 5.71 (1H, s, $=CH_b$), 4.77 (1H, s, C(O<u>H</u>)=C) 2.52 (3H, s, $COCH_3$). ^{13}C-NMR (300 MHz, $CDCl_3$): 189.0 (C=O), 135.7 (<u>C</u>(OH)=C113.2 ($=\underline{C}H_2$), 31.70 ($CO\underline{C}H_3$).

2.2.3. trans-[Ru(tmphen)(L1)Cl_2] (**3**)**:** Yield: 0.092 g (13.1%). Elem. Anal. Calcd. For $C_{33}H_{31}Cl_2N_5O_2Ru$: C, 56.49; H, 4.45; N, 9.98. Found: C, 56.44; H, 4.40; N, 9.96. UV-Vis in CH_2Cl_2 [λ_{max}/nm (ε_{max}/ $M^{-1}cm^{-1}$)]: 271 (28.4×10^3), 321 (6.65×10^3), 381 (4.23×10^3), 510 (2.95×10^3). IR (KBr, cm^{-1}): 1439 (*v* N=N), 1611(*v* C=N), 1673 (*v* C=O). ^{1}H-NMR (300 MHz, $CDCl_3$): 8.11 (2H, d, H3), 8.01 (2H, d, H1), 7.81 (3H, m, H4, H5), 7.67 (1H, s, tmphen), 7.60 (4H, m, H2, tmphen), 7.17 (1H, s, tmphen), 5.93 (1H, s, =CHa), 5.70 (1H, s, =CHb), 4.70 (1H, s, C(O<u>H</u>)=C), 2.87 (3H, s, $COCH_3$), 2.60 (6H, s , tmphen-CH_3), 2.10 (3H, s , tmphen-CH_3), 2.10 (3H, s , tmphen-CH_3), ^{13}C-NMR (300 MHz, $CDCl_3$): (<u>C</u>(OH)=C), 113.18 ($=\underline{C}H_2$), 30.3 ($COCH_3$) , 18.10 (tmphen-CH_3), 18.08 (tmphen-CH_3), 14.63 (tmphen-CH_3), 14.55 (tmphen-CH_3).

2.2.4. trans-[Ru(dmeb)(L2)Cl_2] (**4**)**:** Yield: 0.242 g (36%). Elem. Anal. Calcd. for $C_{29}H_{27}Cl_2N_5O_4Ru$: C, 51.11; H, 3.99; N, 10.28. Found: C, 51.02; H, 3.84; N, 10.26. UV-Vis in CH_2Cl_2 [λ_{max}/nm (ε_{max}/ $M^{-1}cm^{-1}$)]: 267 (26.0×10^3), 369 (5.3×10^3), 502 (0.50×10^3). IR (KBr, cm^{-1}): 1455 (*v* N=N), 1627 (*v* C=N), 1672 (*v* C=O), 1692 (*v* C=O). ^{1}H-NMR (300 MHz, $CDCl_3$): 8.11 (2H, d, H3), 7.74 (3H, m, H4, H5), 7.42 (3H, m, dmeb), 6.98 (1H, d, H1), 6.54 (2H, d, H2), 6.42 (1H, d, dmeb), 6.4 (2H, m, dmeb), 4.04 (6H, s, OCH_3), 2.84 (3H, s, $COCH_3$), 2.74 (3H, s, $COCH_3$). ^{13}C-NMR (300 MHz, $CDCl_3$): 195.4 (C=O), 189.22 (C=O), 56.40 (OCH_3), 56.38 (OCH_3), 30.2 ($COCH_3$), 27.3 ($COCH_3$).

2.2.5. trans-[Ru(phen)(L2)Cl_2] (**5**)**:** Yield: 0.199 g (30.8%). Elem. Anal. Calcd. for $C_{29}H_{23}Cl_2N_5O_2Ru$: C, 53.96; H, 3.59; N, 10.85. Found: C, 53.79; H, 3.66; N, 10.94. UV-Vis in CH_2Cl_2 [λ_{max}/nm (ε_{max}/ $M^{-1}cm^{-1}$)]: 318 (26.4×10^3), 380 (14.82×10^3), 512 (12.35×10^3). IR (KBr, cm^{-1}): 1449 (*v* N=N), 1588 (*v* C=N), 1678 (*v* C=O), 1700 (*v* C=O). ^{1}H-NMR (300 MHz, $CDCl_3$): 8.33 (1H, d, phen), 8.32 (1H, d, phen), 8.16 (3H, m, H3, phen), 7.97 (1H, d, phen), 7.88 (2H, d, H1), 7.80 (1H, t, H5), 7.70 (2H, d, H2), 7.60(2H, t, H4), 7.54 (4H, m, phen), 2.88 (3H, s, $COCH_3$), 2.74 (3H, s, $COCH_3$). ^{13}C-NMR (300 MHz, $CDCl_3$): 198.4 (C=O), 192.3 (C=O), 29.2 ($COCH_3$), 26.8 ($COCH_3$).

2.2.6. trans-[Ru(tmphen)(L2)Cl_2] (**6**)**:** Yield: 0.243 g (34.5%). Elem. Anal. Calcd. for $C_{33}H_{31}Cl_2N_5O_2Ru$: C, 56.49; H, 4.45; N, 9.98. Found: C, 56.39; H, 4.41; N, 9.88. UV-Vis in CH_2Cl_2 [λ_{max}/nm (ε_{max}/ M^{-1} cm^{-1})]: 271 (28.48×10^3), 323 (6.04×10^3), 383 (3.96×10^3), 506 (3.08×10^3). IR (KBr, cm^{-1}): 1444 (*v* N=N), 1617 (*v* C=N), 1699 (*v* C=O), 1704 (*v* C=O). ^{1}H-NMR (300 MHz, $CDCl_3$): 8.20 (2H, d, H3), 8.12 (2H, d, H2), 8.02 (2H, m, tmphen), 7.81 (1H, t, H5), 7.70 (3H, m , H1, tmphen), 7.61 (2H, t, H4), 7.11 (1H, d, tmphen), 2.88 (3H, s,

$COCH_3$), 2.76 (3H, s, $COCH_3$), 2.62 (6H, s , tmphen-CH_3), 2.12 (3H, s , tmphen-CH_3), 2.05 (3H, s , tmphen-CH_3). ^{13}C- NMR (300 MHz, $CDCl_3$): 197.14 (C=O) , 189.07 (C=O), 30.2 ($CO\underline{C}H_3$), 26.9 ($CO\underline{C}H_3$), 18.12 (tmphen-CH_3), 18.06 (tmphen-CH_3), 14.66 (tmphen-CH_3), 14.57 (tmphen-CH_3).

2.3. Instrementation

NMR spectra were obtained using a Bruker Avance 300 spectrometer. Microanalytical data were collected on an Eurovector E.A.3000 instrument using thin sample-tubes. Infrared spectra were recorded on JASCO 420. UV–Vis spectral studies were performed using a TIDAS Fiberorptic diode array spectrometer. Cyclic voltammetric measurements were carried out using a BAS CV-27 voltammograph.. A platinum wire working electrode, a platinum wire auxiliary electrode and Ag wire reference electrode were used in a standard three-electrode configuration. Tetrabutylammonium hexafluorophosphate (0.1 M) was used as the supporting electrolyte; the scan rate used was 0.1V s^{-1} in acetonitrile under N_2 atmosphere. Referencing was done with the addition of 1 mg of ferrocene [16, 17]. The spectroelectrochemistry of complex **3** was investigated as a representative using an optically transparent thin layer electrode (OTTLE) cell [18].

2.4. Crystallography

Details of crystal analysis, data collection and structure refinement data for complexes **3** and **7** are given in Table 1. Crystals mounting was done on glass fibers with epoxy cement. Single crystal data collections were performed on Xcalibur/Oxford Diffractometer using Mo tube (λ = 0.71073 Å) as X-ray source. CrysAlis Pro software was used for data collection, absorption correction and data reduction to give SHELX-format-*hkl* files [19]. The structures were solved and refined using SHELXTL program package [20]. In the crystal structure of complex 7, two restraints were applied; the anisotropic displacement parameters of the atoms C16 and C17 in the direction of C16-C17 bond are restrained to be equal, similarly, these parameters of atoms C16 and C13 are restrained to be equal along C16-C13 bond.

2.5. Procedure for Catalytic Hydrogenation of Cinnamaldehyde

The liquid-phase hydrogenation of cinnamaldehyde (1:1 *cis*-to-*trans* mixture) was performed in a stainless steel hydrogenator (Parr-4842) equipped with a Waltow-945 unit to control the temperature of reactions and the stirring rate. The reaction solution, prepared by dissolving the desired amounts of **3** (0.040 g), potassium hydroxide (0.047) and cinnamaldehyde (0.80 g) in 100 ml 2-propanol, is placed in the reaction vessel and the hydrogenator is tightly closed. The reactor temperature is adjusted at 86 ^{o}C before admitting the hydrogen gas at 3 bars. Samples from the reaction solution are taken at various time intervals and analyzed by gas chromatography (Agilent, FID, 30-m crosslinked FAFF capillary column).

3. Results and Discussion

3.1. Synthesis

Treatment of azoimine ligand has a terminal acetylene group (L: Ph–NH-N=C($COCH_3$)-NH–PhC≡CH) with $RuCl_3.3H_2O$ in refluxing absolute ethanol offered a catalytic hydration of the triple bond *via* Markovnikov addition to corresponding enol (L1: Ph–NH-N=C($COCH_3$)-NH–PhC(OH)=CH_2) and ketone (L2: Ph–NH-N=C($COCH_3$)-NH–Ph($COCH_3$) in addition to trace amount of the vinyl chloride (L3: Ph–NH-N=C($COCH_3$)-NH–PhC(Cl)=CH_2) (Scheme1). The proposed mechanism for the hydration of acetylene involves the dissociation of one chloride ligand from starting Ru(III)$Cl_3.nH_2O$ complex, generating Ru(III)$Cl_2.nH_2O$ active species. The catalytic hydration starts by the activation of the acetylene group through Ru(III)-π interactions [21]. Enol and keto form may have obtained by the hydration of the coordinated alkyne by addition of one water molecule to the internal position of the triple bond [22, 23]. The vinylchloride complex is believed to have been generated by the nucleophilic attack of the dissociated chloride ligand on the activated acetylene group.

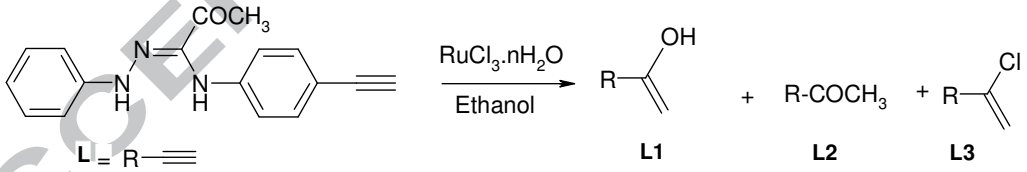

Scheme1: catalytic hydration products

Mixed-ligand ruthenium complexes built from α-diamine ((N-N) where N-N= 1,10-phenanthroline (phen), 4,4'-dimethoxy-2,2'-bipyridine (dmeb), 1,3,4,7,8-tetramethyl-1,10-phenanthroline (tmphen)] having a general formula of *trans*-[Ru(N-N)(Y)Cl_2] (**1-6**) (where Y =L1, N-N= phen (**1**), dmeb (**2**), tmphen (**3**) and Y=L2, N-N= phen (**4**), dmeb (**5**), tmphen

(**6**)) were achieved by the stepwise addition of equimolar amounts of (L) and N-N ligands to $RuCl_3.3H_2O$ in absolute ethanol (Scheme 2).

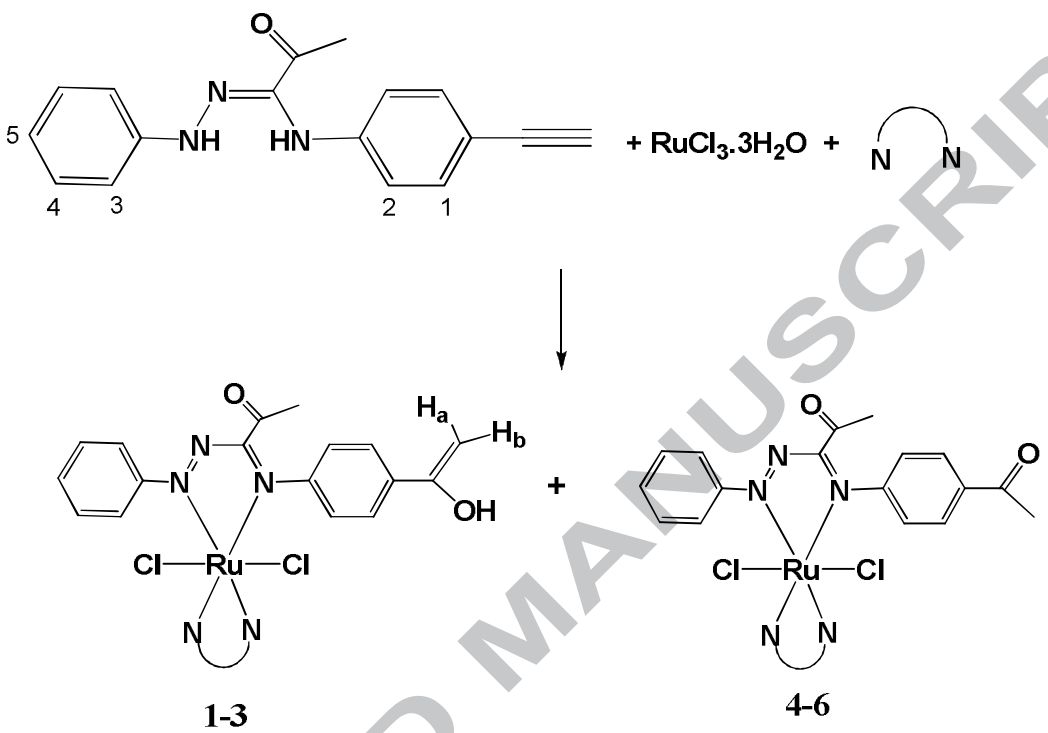

Scheme 2: Synthesis of *trans*-[Ru(N-N)(Y)Cl_2] (**1-6**)

In the carbonyl region of the IR spectra, complexes **1-3** showed an intense band in the range of 1673-1701 cm^{-1} corresponding to the acetyl group while complexes **4-6** exhibited two bands (1672-1699 and 1792-1704 cm^{-1}) for the two acetyl groups types. Complexes **1-3** were confirmed by the appearance of two doublets for the vinyl protons (H_a and H_b) at δ 5.93-5.94 and 5.67-5.716 ppm, one exchangeable singlet for the hydroxyl proton (4.70-4.77 ppm) and one negative signal for the vinyl carbon at 113.0-113.2 ppm in their ^{13}C-NMR (distortionless enhancement by polarization transfer (DEPT-135)) spectra. In the ^{1}H NMR spectra of complexes **4-6**, two CH_3 singlets in the ranges of 2.84-2.88 ppm and 2.74-2.76 ppm are observed. The carbons of these methyl groups are presented in the ranges of 29.2-

30.2 and 26.8-27.3 ppm in the ^{13}C NMR spectra. In addition, two signals in the ranges of 198.4-194.4 and 189.1-189.3 ppm corresponding to the carbonyl carbons are also shown.

3.2. Crystal Structures

Single crystals of the complexes **3** and **7** are obtained by slow diffusion of hexane into a dichloromethane solution of the complexes. Selected bond distances and bond angles are given in Table 2. The ORTEP drawings with numbering schemes of these complexes are shown in Figure 1 and Figure 2, respectively. The geometry around the Ru atom of complex **3** and **7** occupies a *pseudo* octahedral coordination which consists of two *trans* chloride ligands and four nitrogen donor atoms. For complex **3**, all the atoms in the side-chain C(17), C(16) and O(2) are coplanar. The bond length C(17)–C(16) of 1.434(17) Å is comparable to distinct C–C bonds in asymmetric enolized 1,3-diones [24-26]. The C13-C16 bond length of 1.50 Å, is a typical distance for C-C single bond. Furthermore, the dihedral angle of 26.81 between the enol plane and the plan of the benzene ring attached to the azoimine skeleton indicates minimal conjugation between the two groups. The enol O(2)-C(16) distance is 1.478(17) Å while the ketone O(1)-C(8) bond distance is 1.176(11) Å. The bite-angles for the five membered ring for coordinated L1 N(4)-Ru(1)-N(5), 76.9(3)° and imine ligand tmphen N(1)-Ru(1)-N(3), are almost equivalent.

The average Ru–N(azo) and Ru–N(methine) distances of the azomethine ligand of complex 7 is 1.983 Å. The Ru–N(bpy) bond length of 2.127 Å which is slightly shorter than the Ru^{II}-bpy bond in *trans*-[Ru(bpy)(L2)Cl_2] (average, 2.147 Å) [15]. The atoms in the side-chain C(17), C(16) and Cl(3) are coplanar. The C(17)–C(16) bond length in complex **7** is 1.314(9) Å is shorter than the corresponding bond in complex **3**. Furthermore, the dihedral angle between the vinyl chloride plane and the phenyl ring attached to the azoimine skeleton is 19.0° indicating minimal conjugation between the two groups.

The Ru–N(tmphen) bond for in complex **3** (2.1165 Å) are slightly shorter than the Ru–N(bpy) bonds (2.127 Å) in **7** revealing that there is no significant difference in the strength of the coordination for the two ligands. The average Ru–Cl bond lengths (for **3**: 2.358, **7**: 2.3619 Å) are comparable to those reported for similar systems (2.389–2.401 Å) [11-15].

3.3. Electrochemistry

The Ru(III/II) couple of complexes **1**-**6** was tested by cyclic voltammetric measurements and the results are presented in Table 3. The cyclic voltammogram of complex **3** is shown in Figure 3 and exhibits a reversible oxidative response around 0.60 V *vs.* $Cp_2Fe^{0/+}$ which has been assigned to Ru(III/II) oxidation. The irreversible couple at negative potential is assigned to the ligand (0/-1) reduction which, however is less anodic than the corresponding peak of the keto complex **6**.

Table 3 shows that the half-wave potential of the phenanthroline complexes was shifted anodically by ~ 40 mV compared to those observed in the bipyridine complexes. This may indicates that the donor ability of phenanthroline is slightly weaker than that of bipyridine. The Ru(III/II) couple is slightly affected by changing the substituent on the phenanthroline and 2,2'-bipyridine ligands and is shifted to more negative potentials upon replacing the hydrogen atoms by donating methyl group (Table 3).

3.4 Electronic Structure

As a representative example, Figure 4 shows the UV–Vis spectrum of complex **3** in dichloromethane. The lowest energy band at 512 nm was assigned to metal ligand charge transfer (MLCT). The high intensity and energy band at 284 nm may be attributed to a ligand-to-ligand charge transfer LLCT (π-π* (phenyl ring) and n-π* (azomethine (C=N)) transitions. Figure 4 shows the stepwise oxidation of complex **3** in dichloromethane to $\mathbf{3}^{+}$, there is a decrease in the intensity of the MLCT centered at 512 nm and a grow of two new bands at 450 nm and 650 nm. The latter band may result from the Cl^{-} (pπ)→Ru(III)(dπ) ligand to metal charge transfer (LMCT), while the former may assigned to L1(π) → Ru(III)(dπ) LMCT.

Stepwise reduction at negative potentials for complex **3** in dichloromethane to $\mathbf{3}^{-}$ causes the the azoimine-targeted MLCT absorption band to disappear (Figure 5) and a very intense band in the UV and NIR-region to appear. The intense band in the NIR region is assigned to L^{-}(π)→Ru(dπ*) LMCT while the bands around 450 and 350 nm may have resulted from LLCT.

3.5. Hydrogenation of Cinnamaldehyde (CALD)

Cinnamaldehyde has been selected as a model substrate for hydrogenation. Scheme 3 represents the various hydrogenation routes that CALD may undergo [27]. The hydrogenation of the C=O bond yields the highly desirable cinnamyl alcohol (CALC) while that of the C=C bond produces the less desirable hydrocinnamaldehyde (HCALD). Consecutive hydrogenation of CALC and HCALD gives phenyl propanol (PP). Complex **3** was tested as a representative example with respect to the catalytic activity of the Ru(II) complexes for the hydrogenation of cinnamaldehyde in the liquid phase.

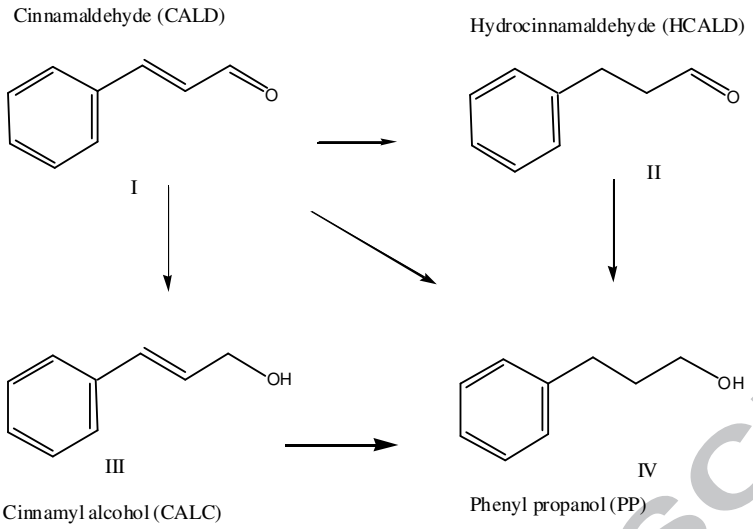

Scheme 3**:** Cinnamaldehyde hydrogenation.

The progress of cinnamaldehyde hydrogenation using complex **3** as a catalyst is depicted in Figure 6. The ratio of substrate (CALD): co-catalyst ($NaOCH_3$): catalyst (**3**) is 68:22:1. The reaction was conducted at 86 ^oC under hydrogen pressure of 4 atm. In the first 120 min. of the reaction, CALD concentration changes very slowly. This is the stage where the actual catalyst is being produced. The hydrogenation of CALD follows thereafter a first order kinetics with a rate constant of 1.56×10^{-3} min^{-1}. The formation of CALC obeys also first-order kinetics with a rate constant of 4.00×10^{-4} min^{-1}. There is no indication that CALC undergoes consecutive hydrogenation to PP, on contrary to HCALD whose concentration goes through a maximum, as expected for intermediates, after 500 min. of reaction. The catalytic efficiency of complex **3** is however very small and the turn-over-frequency (TOF, number of substrate molecules reacted per catalytic site per time) after 550 min. of reaction is 3 h^{-1}. This TOF is very small compared to that observed for $Ru(bipy)(C_6H_5N{=}N{-}C(COCH_3){=}NC_6H_4SPh)Cl_2$ that contains a thiophenyl group instead of the enol functionality in the azoimine ligand for which a TOF value of 42 h^{-1} was observed at a substrate: catalyst ratio of 84:1 [28]. In addition to the low activity (expressed by conversion) of complex **3** (Table 4), the selectivity to CALC is also rather small (~33-37%).

The TOF for the formation of CALC is thus only 1 h^{-1} compared to 40 h^{-1} observed for the other catalysts reported for which the CALC selectivity reached 95%.

Conclusion

The reaction of azoimine ligand bearing a terminal acetylene group, L= Ph–NH-N=C($COCH_3$)-NH–C_6H_4C≡CH, with $RuCl_3.3H_2O$ in absolute ethanol resulted in the catalytic hydration of the terminal acetylene group *via* Markovnikov selectivity to the corresponding enol (L1) , ketone (L2) in addition to trace amount of the vinyl chloride (L3). Mixed-ligand ruthenium complexes having the general formula *trans*-[Ru(N-N)(Y)Cl_2] (**1**-**6**) (Y = L1, N-N= 4,4'-dimethoxy-2,2'-bipyridine; dmeb (**1**), 1,10-phenanthroline; phen (**2**), 3,4,7,8-tetramethyl-1,10-phenanthroline; tmphen (**3**) and Y = L2, N-N= dmeb (**4**),; phen (**5**), tmphen (**6**)) were synthesized. The crystal structures of *trans*-[Ru(tmphen)(L1)Cl_2] (**3**) and *trans*-[Ru(bpy)(L3)Cl_2] (**7**) were determined. The UV-Vis spectra of **3**, $\mathbf{3}^+$ and $\mathbf{3}^-$ in dichloromethane has been obtained and discussed.

Acknowledgements

M. Al-Noaimi would like to thank the Hashemite University (Jordan) for research support.

Appendix A. Supplementary data

CCDC 1439361 (for **3**) and 1439360 (for **7**) contain the supplementary crystallographic data for the two complexes. These data can be obtained free of charge via http://www.ccdc.cam.ac.uk/conts/retrieving.html, or from the Cambridge Crystallographic Data Centre, 12 Union Road, Cambridge CB2 1EZ, UK; fax: (+44) 1223-336-033; or e-mail: deposit@ccdc.cam.ac.uk.

References

1. R. Casado, M. Contel, M. Laguna, P. Romero, S. Sanz, J. Am. Chem. Soc. 125 (2003) 11925.

2. S. Sanz, L.A. Jones, F. Mohr, M. Laguna, Organometallics 26 (2007) 952.

3. J. March, Advanced Organic Chemistry, 4th ed.; Wiley: New York, 1992.

4. M.M.T. Khan, S.B. Halligudi, S. Shukla, J. Mol. Catal. 58 (1990) 299.

5. J. Blum, H. Huminer, H. Alper, J. Mol. Catal. 75 (1992) 153.

6. K. Imi, K. Imai, K. Utimoto, Tet. Lett. 28 (1987) 3127.

7. W.D. Harman, J.C. Dobson, H. Taube, J. Am. Chem. Soc. 111(1989) 3061.

8. L.W. Francisco, D.A. Moreno, J.D. Atwood, Organometallics 20 (2001) 4237.

9. X. Wu, D. Bezier, C. Darcel, Adv. Synth. Catal. 351 (2009) 367.

10. T. Suzuki, M. Tokunaga, Y. Wakatsuki, Org. Lett. 3 (2001) 735.

11. M. Al-Noaimi, M. El-khateeb, S. Haddad, M. Sunjuk, R. Crutchley, Polyhedron 27 (2008) 3239

12. M. Al-Noaimi, R.J. Crutchley, M. AlDamen, A. Rawashdeh, M.A. Khanfar, K. Seppelt, Polyhedron 30 (2011) 2075.

13. M. Al-Noaimi, M.A. AlDamen, Inorg. Chim. Acta 387 (2012) 45.

14. M. Al-Noaimi, M. El-khateeb, I. Warad, S.F. Haddad, Inorg. Chim. Acta 400 (2013) 20.

15. M. Al-Noaimi, F.F. Awwadi, A. Mansi, S. Abdel-Rahman, A. Hammoudeh, I. Warad, Spectrochim. Acta, Part A: Mol. Biomol. Spec. 135 (2015) 828.

16. M. Krejcik, M. Danek, F. Hartl, J. Electroanal. Chem. 317 (1991) 179.

17. C. Nataro, A.N. Campbell, M.A. Ferguson, C.D. Incarvito, A.L. Rheingold, J. Organomet. Chem. 673 (2003) 47.

18. T. Gennett, D.F. Milner, M.J. Weaver, J. Phys. Chem. 89 (1985) 2787.

19. CrysAlisPro, Agilent Technologies, Version 1.171.35.11 (Release 16–05–2011 CrysAlis171.NET) (Compiled May 16 2011, 17:55:39).

20. SHELXTL (XCIF, XL, XP, XPREP, XS), version 6.10, Bruker AXS Inc.: Madison, WI, 2002.

21. J. Halpern, B.R. James, A.L. W. Kemp, J. Am. Chem. Soc. 83(1961) 4097.

22. I.K. Meier, J.A. Marsella, J. Mol. Cat. 78 (1993) 31.

23. C.M. Krauter, A.S.K. Hashmi, M. Pernpointner. Chem. Cat. Chem. 2 (2010) 1226

24. W. Bell, J.A. Crayston, C. Glidewell, M.A. Mazid, M.B. Hursthouse, J. Organomet. Chem. 434 (1992) 115.

25. A. Mostad, U. Pedersen, P.B. Rasmussen, S. Lawesson, Acta Chem. Scand. 37b (1983) 901.

26. L.A.M. Baxter, A.J. Blake, G.A. Heath, T.A. Stephenson, Acta Cryst. C, Crystal Struct. Comm. 46 (1990) 508.

27. I. Warad, M. Al-Noaimi, O.S. Abdel-Rahman, M. AlDamen, B. Hammouti, T.B. Hadda, Polyhedron 63 (2013)182.

28. H.A. Ali, M. Al-Noaimi, S.S. Mahmoud, A.Y. Hammoudeh, Jord. J. Chem. 10 (2015) 58.

Table 1. Crystal data and structure refinement parameters for **3** and **7**.

	3	**7**
Empirical formula	$C_{33}H_{31}C_{l2}N_5O_2Ru$	$C_{27}H_{22}Cl_3N_5ORu$
Formula weight	701.60	639.92
Temperature	293(2) K	293(2) K
Wavelength	0.71073 Å	0.71073 Å
Crystal system	Monoclinic	Triclinic
Space group	P 1 21/n 1	P-1
Unit cell dimensions	a=13.6384(14),b=15.8352(11)Å c=15.8432(16)Å α= 90, β= 06.362(12)° , γ= 90°	a=8.8814(7) Å, b=12.1926(10)Å,. c=13.8803(13)Å, α=80.964(7),β=77.056(7),γ= 72.185(7)°
Volume	3283.0(5) $Å^3$	1388.3(2) $Å^3$
Z	4	2
Density (calculated)	1.419 Mg/m^3	1.531 Mg/m^3
Absorption coefficient	0.677 mm^{-1}	0.883 mm^{-1}
F(000)	1432	644
Theta range for data collection	2.97 to 25.00° .	3.03 to 26.30°
Index ranges	-16≤h≤15, -18≤k≤16, -18≤l≤18	-11≤h≤9, -15≤k≤10, -17≤l≤17
Reflections collected	15471	10061
Independent reflections	5769 [R(int) = 0.0731]	5632 [R(int) = 0.0533]
Completeness to theta = 26.30°	99.8 %	99.9 %
Absorption correction	Semi-empirical from equivalents	Semi-empirical from equivalents
Max. and min. transmission	1.00000 and 0.75059	1.0 and 0.98819
Refinement method	Full-matrix least-squares on F^2	Full-matrix least-squares on F^2
Data / restraints / parameters	5769 / 0 / 388	5632 / 2 / 334
Goodness-of-fit on F^2	1.036	0.993
Final R indices [I>2sigma(I)]	R1 = 0.0787, wR2 = 0.1578	R1 = 0.0654, wR2 = 0.1058
R indices (all data)	R1 = 0.1553, wR2 = 0.2013	R1 = 0.1393, wR2 = 0.1368
Largest diff. peak and hole	1.000 and -0.433 e.$Å^{-3}$	0.448 and -0.638 e.$Å^{-3}$

$R_1 = \Sigma||F_o| - |F_c||/\Sigma|F_o|$; $wR_2 = \{\Sigma[\ w(F_o^2 - F_c^2)^2]/\ \Sigma\ [w(F_o^2)^2]\}^{1/2}$

Table 2. Selected bond Lengths and angles for complexes **3** and **7**

3		**7**	
Bond lengths(Å)			
Ru(1)-N(1)	1.941(6)	Ru(1)-N(1)	1.954(5)
Ru(1)-N(3)	2.006(6)	Ru(1)-N(3)	2.012(5)
Ru(1)-N(5)	2.117(7)	Ru(1)-N(5)	2.103(5)
Ru(1)-N(4)	2.166(6)	Ru(1)-N(4)	2.151(5)
Ru(1)-Cl(2)	2.352(2)	Ru(1)-Cl(1)	2.3545(17)
Ru(1)-Cl(1)	2.369(2)	Ru(1)-Cl(2)	2.3694(16)
O(1)-C(8)	1.176(11)	N(1)-N(2)	1.320(6)
O(2)-H(2C)	0.8200	N(1)-C(1)	1.445(8)
C(17)-C(16)	1.434(17)	N(5)-C(27)	1.341(8)
O(2)-C(16)	1.478(17)	C(16)-C(17)	1.314(9)
N(1)-N(2)	1.316(8)	C(16)-Cl(3)	1.745(8)
N(3)-C(7)	1.317(10)		
Bond angles (°)			
N(1)-Ru(1)-N(3)	76.4(3)	N(1)-Ru(1)-N(3)	75.8(2)
N(1)-Ru(1)-N(5)	102.1(3)	N(1)-Ru(1)-N(5)	102.8(2)
N(3)-Ru(1)-N(5)	172.5(3)	N(3)-Ru(1)-N(5)	175.7(2)
N(1)-Ru(1)-N(4)	175.3(2)	N(1)-Ru(1)-N(4)	175.26(19)
N(3)-Ru(1)-N(4)	105.3(3)	N(3)-Ru(1)-N(4)	105.7(2)
N(5)-Ru(1)-N(4)	76.9(3)	N(5)-Ru(1)-N(4)	76.00(19)
N(1)-Ru(1)-Cl(2)	93.75(19)	N(1)-Ru(1)-Cl(1)	94.56(15)
N(3)-Ru(1)-Cl(2)	89.0(2)	N(3)-Ru(1)-Cl(1)	89.95(14)
N(5)-Ru(1)-Cl(2)	83.74(18)	N(5)-Ru(1)-Cl(1)	86.09(14)
N(4)-Ru(1)-Cl(2)	90.72(17)	N(4)-Ru(1)-Cl(1)	89.95(13)
N(1)-Ru(1)-Cl(1)	91.65(19)	N(1)-Ru(1)-Cl(2)	92.32(15)
N(3)-Ru(1)-Cl(1)	93.0(2)	N(3)-Ru(1)-Cl(2)	93.16(15)
N(5)-Ru(1)-Cl(1)	94.32(18)	N(5)-Ru(1)-Cl(2)	90.97(14)
N(4)-Ru(1)-Cl(1)	83.87(18)	N(4)-Ru(1)-Cl(2)	83.14(13)
Cl(2)-Ru(1)-Cl(1)	174.54(8)	Cl(1)-Ru(1)-Cl(2)	172.97(6)
O(1)-C(8)-C(7)	119.8(10)		

Table 3: Electrochemical data for **1-6** in CH_2Cl_2/ $TBAPF_6$ (0.1 mM); potentials are given relative to the ferrocene/ferrocenium standard at v = 0.1 V/s

Complex	[a]Ru(II/III)(V)	[b]Azo(0/-1)(V)
trans-[Ru(bpy)(L1)Cl_2]**[18]**	0.60	-1.07
1	0.58	-1.14
2	0.59	-1.18
3	0.60	-1.17
trans-[Ru(bpy)(L2)Cl_2]**[18]**	0.62	-1.06
4	0.63	-1.19
5	0.66	-1.11
6	0.65	-1.12

[a] reversible wave.

[b] irreversible wave.

Table 4: The results of cinnamaldehyde hydrogenation using **3**

time (min)	HCALD%	PP%	CALD%	CALC%	conv%	S_{CALC}%
0	0	0	100.00	0	0	-
60	0.59	0.16	97.90	1.35	2.10	64.41
120	2.58	0.44	92.47	4.50	7.53	59.80
180	3.47	0.78	88.45	7.30	11.55	63.16
240	4.24	1.36	84.19	10.20	15.81	64.56

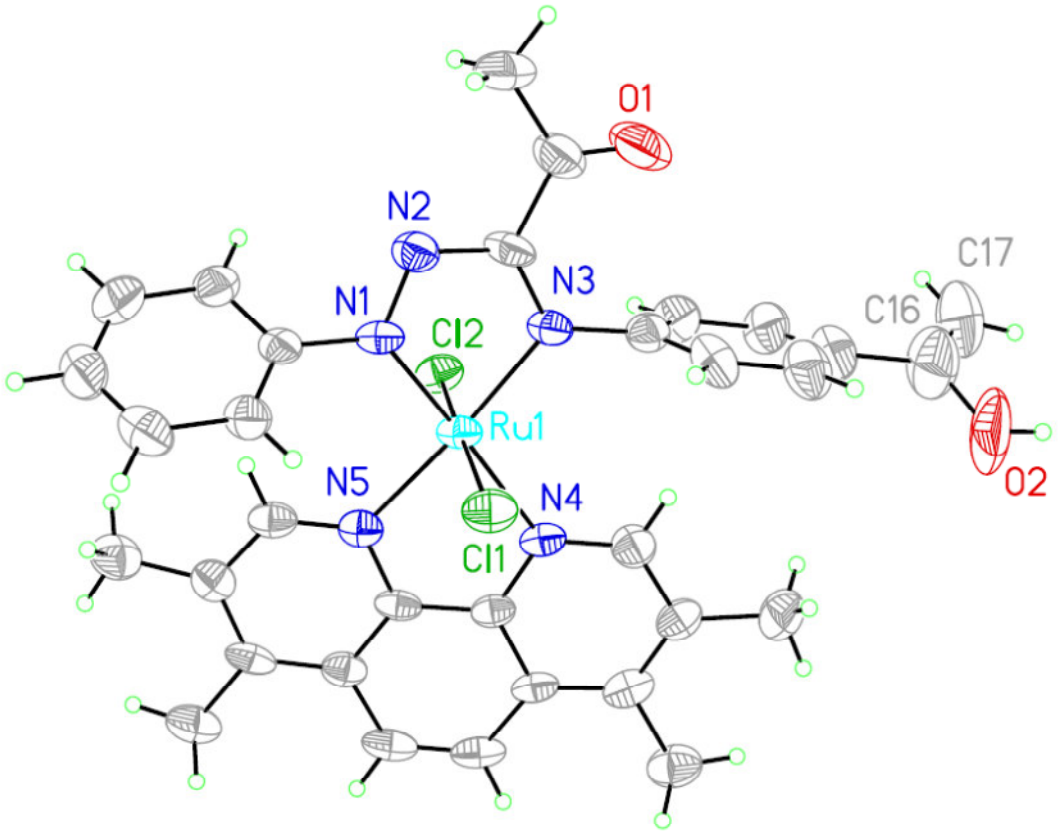

Figure 1:.ORTEP drawing of **3**.Thermal ellipsoids plots are reported at 30% probability.

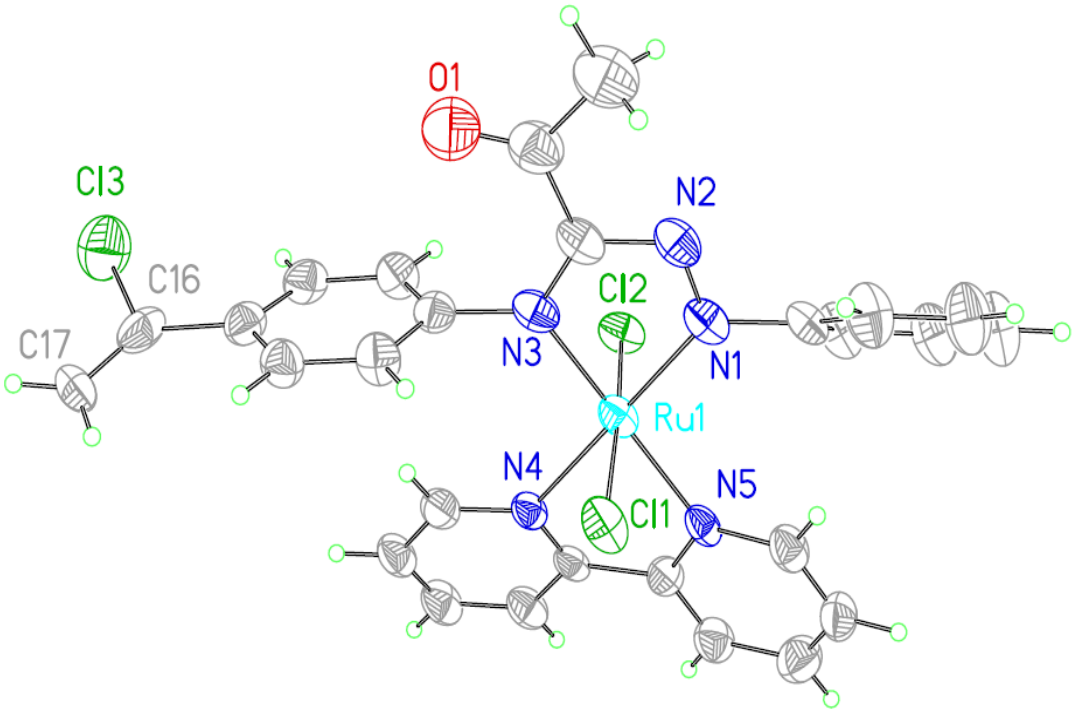

Figure 2. ORTEP drawing of **7**. Thermal ellipsoids plots are reported at 30% probability.

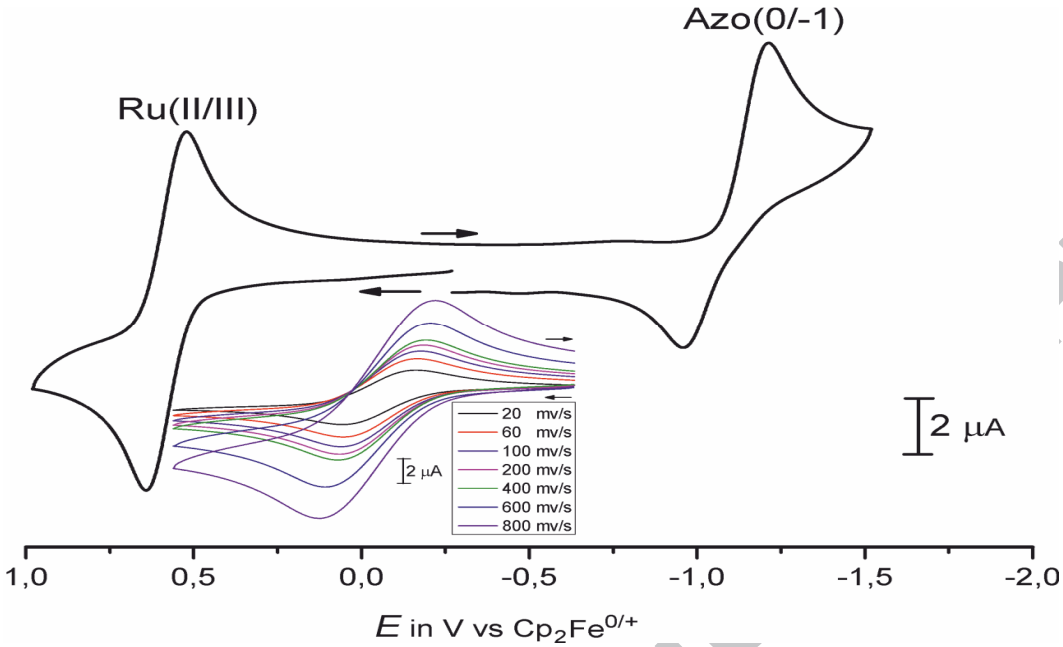

Figure 3: Cyclic voltammogram of complex **1** vs. $Cp_2Fe^{0/+}$ ($TBAPF_6$, 0.1M, dichloromethane, 25˚C). Inset shows the Ru(II/III) at different scans rate.

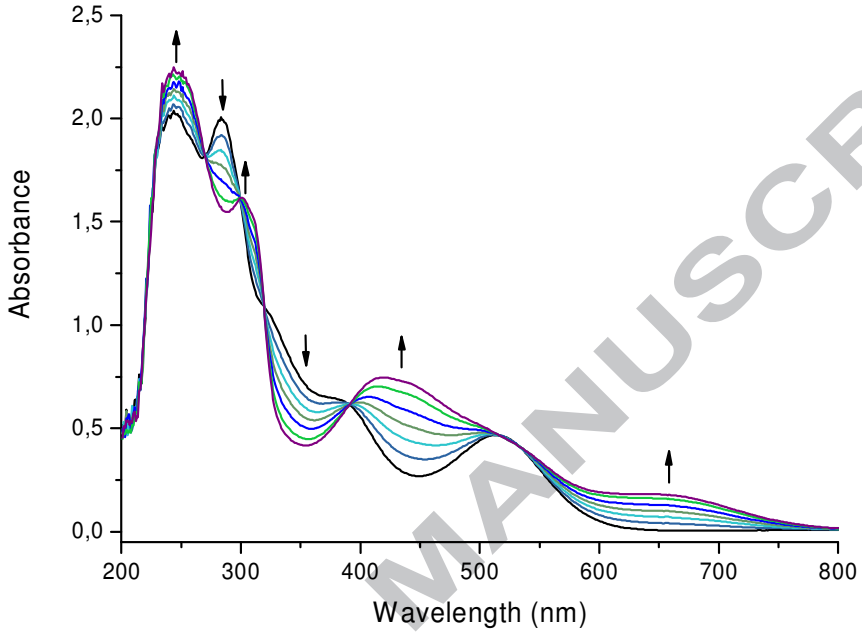

Figure 4: Oxidation spectroelectrochemistry of complex **3** in dichloromethane

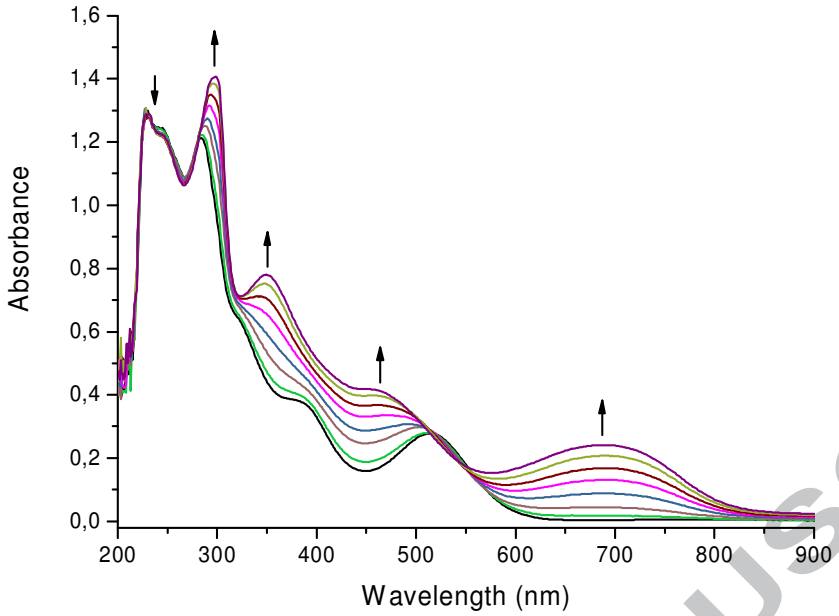

Figure 5: Reduction spectroelectrochemistry of complex **3** to **3**$^{-}$ in dichloromethane

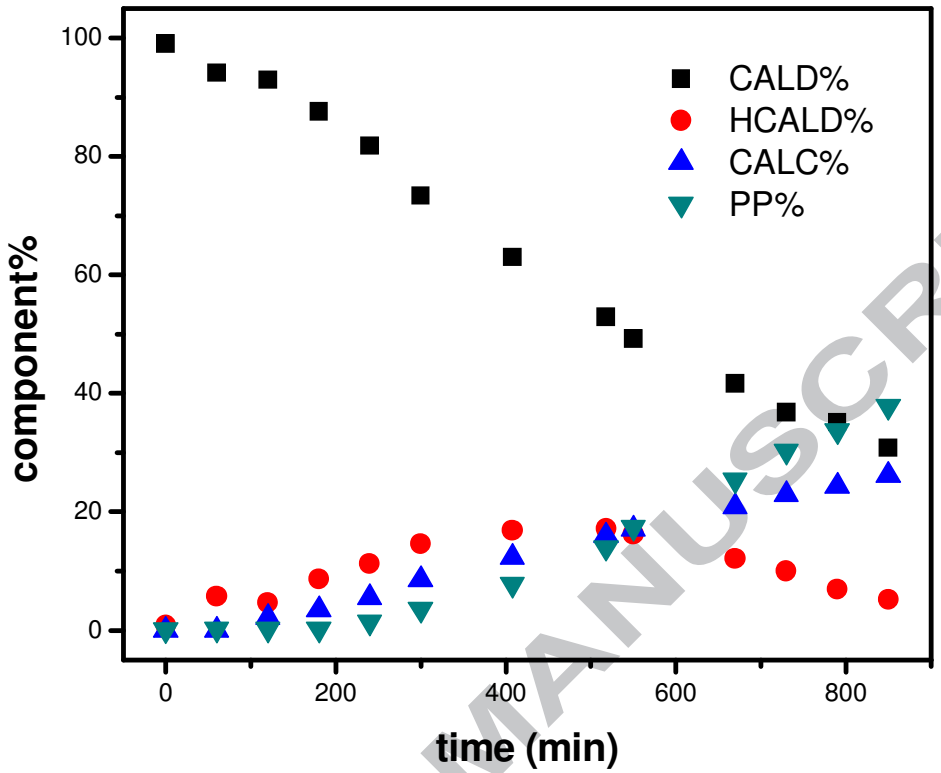

Figure 6: The progress of the catalytic hydrogenation of CALD, Cinnamaldehyde: 0.6081 g in 100 mL i-propanol, 0.046 M; Co-catalyst: $NaOCH_3$, 0.0810 g, 1.5×10^{-2} M; Catalyst: complex **3**, 0.0424 g, 6.8×10^{-4} M; Temperature: 86°C, Hydrogen pressure: 4 atm, reactant: co-cat : cat = 68 : 22 : 1

Refluxing azoimine ligand (L= $C_6H_5N{=}NC(COCH_3){=}NC_6H_4C{\equiv}CH$) with $RuCl_3.3H_2O$ in ethanol resulted in catalytic hydration of the terminal acetylene group to the enol form $C_6H_5N{=}N{-}C(COCH_3){=}NC_6H_4C(OH){=}CH_2$ (L1), the ketone form $C_6H_5N{=}NC(COCH_3){=}NC_6H_4COCH_3$ (L2) and the vinyl chloride: $C_6H_5N{=}N{=}C(COCH_3){=}N{-}C_6H_4C(Cl){=}CH_2$ (L3) *via* Markovnikov selectivity. Ruthenium complexes of the formula *trans*-[Ru(N-N)(Y)Cl_2] (Y = L1, N-N = 4,4'-dimethoxy-2,2'-bipyridine; dmeb (**1**), 1,10-phenanthroline; phen (**2**), 3,4,7,8-tetramethyl-1,10-phenanthroline; tmphen (**3**), Y = L2, N-N = dmeb (**4**), phen (**5**), tmphen (**6**)) were made from L, N-N ligands and $RuCl_3.3H_2O$. Complexes **1-6** were characterized by spectroscopic techniques (IR, UV–Vis, ^{1}H-, ^{13}C-NMR, DEPT-135) and electrochemistry. The crystal structures of *trans*-[Ru(tmphen)(L1)Cl_2] (**3**) and *trans*-[Ru(bpy)(L3)Cl_2] (**7**) were determined and found to have distorted octahedral geometry. The catalytic activity of **3** towards the hydration of cinnamaldehyde is described

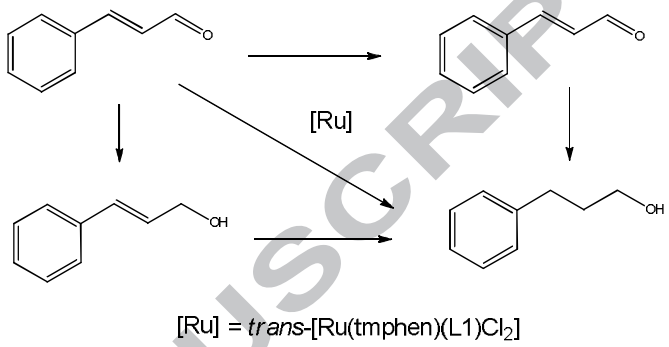

[Ru] = *trans*-[Ru(tmphen)(L1)Cl_2]

Research highlights

- Azoimine- ligand (L) with terminal acetylene.
- Markovnikov hydration of the terminal acetylene in L to enol (L1), ketone (L2) and the vinyl chloride (L3).
- Mixed-ligand ruthenium complexes, trans-[Ru(N-N)(Y)Cl_2] , N-N: α-diamine and Y:L1, L2 and L3.
- Crystal structures of the enol and vinyl chloride form.
- A complex served as hydrogen transfer catalysts for cinnamaldehyde.